Src Promotes Survival and Invasion of Lung Cancers with Epidermal Growth Factor Receptor Abnormalities and Is a Potential Candidate for Molecular-Targeted Therapy

Elaine Lai-Han Leung,[1] Issan Yee-San Tam,[1] Vicky Pui-Chi Tin,[1] Daniel Tsin-Tien Chua,[2] Alan Dart-Loon Sihoe,[4] Lik-Cheung Cheng,[4] James Chung-Man Ho,[3] Lap-Ping Chung,[1] and Maria Pik Wong[1]

Departments of [1]Pathology, [2]Clinical Oncology, and [3]Medicine, University of Hong Kong, Queen Mary Hospital; and [4]Cardiothoracic Surgery Unit, The Grantham Hospital

Abstract

Molecular-targeted therapy using tyrosine kinase inhibitors against epidermal growth factor receptor (EGFR) is an effective therapy for non–small cell lung cancer that harbor EGFR mutations. This study aimed to investigate the role of Src, a close EGFR associator, as a drug target in NSCLC cells with different *EGFR* genomic statuses. Src inhibition was achieved using 4-(4′-Phenoxyanilino)-6,7-dimethoxyquinazolinee (SKI-1) and the specificity of action was verified by RNA interference. The results showed that SKI-1 induced significant apoptosis in a dose-dependent manner in cancer cells with high basal Src activation. Activation of FAK and p130Cas was involved in Src-mediated invasion in SKI-1–sensitive cells. SKI-1 inhibited phosphorylation of EGFR as well as EGFR downstream effectors, such as signal transducers and activators of transcription 3/5, extracellular signal-regulated kinase 1/2 and AKT in the mutant cells but not the wild-type cells. This inhibition profile of EGFR implicates that induction of apoptosis and sensitivity of mutant cells to SKI treatment is mediated by EGFR and EGFR downstream pathways. Cotreatment with SKI-1 and gefitinib enhanced apoptosis in cancer cells that contained *EGFR* mutation and/or amplification. SKI-1 treatment alone induced significant apoptosis in H1975 cells known to be resistant to gefitinib. Src phosphorylation was shown by immunohistochemistry in around 30% of primary lung carcinomas. In 152 adenocarcinomas studied, p-Src was associated with *EGFR* mutations ($P = 0.029$). Overall, the findings indicated that Src could be a useful target for treatment of non–small cell lung cancer. Besides *EGFR* genomic mutations, other forms of *EGFR* and related family member abnormalities such as *EGFR* amplification might enhance SKI sensitivity. (Mol Cancer Res 2009;7(6):923–32)

Introduction

Src is a nonreceptor tyrosine kinase involved in the cross-talk and mediation of a number of signaling pathways (1-3) that promote cell proliferation, adhesion, invasion, migration, metastasis, angiogenesis, and tumorigenesis (4). Elevation of Src protein levels and/or kinase activity have been reported in many human cancers, including those from the breast (5), colon (6), ovary (7), stomach (8), and lung (9-11).

Epidermal growth factor receptor (*EGFR*) mutations are commonly found in non–small cell lung cancer (NSCLC) especially adenocarcinomas from women, East Asians, and nonsmokers. The most common mutations including those from Oriental patients (12, 13) are exon 19 deletion and L858R substitution of the kinase activation domain (14). Targeted therapy using tyrosine kinase inhibitors (TKI) against EGFR is an effective therapy for NSCLC that harbor activating *EGFR* mutations (15, 16). However, acquired resistance to TKI may occur as a result of second *EGFR* mutation (e.g., T790M substitution), *MET* amplification, or activation of alternative survival pathways, such as the KRAS and ErbB3 pathways (17, 18).

Src and EGFR act synergistically through mutual phosphorylation and activation (19-21). Recent studies have shown that Src kinase inhibitors (SKI) can induce apoptosis (22, 23), arrest cell cycle (22), inhibit cell proliferation, invasion, and vascularization (24) in several types of NSCLC cells and/or xenograft models, but there is limited information regarding the *in vivo* activation status of Src in NSCLC. Also, the effects of combined TKI and SKI treatment have not been fully studied. To analyze the potential usefulness of Src kinase inhibition in treating NSCLC, we studied the expression and activation patterns of Src in a panel of human lung cancers, as well as the effects of Src inhibition alone or in combination with EGFR inhibitor on a panel of human NSCLC cell lines with known *EGFR* mutational status, including exon 19 deletion, L858R substitution, L858R and T790M double substitution, and *EGFR* amplification. Src inhibition was achieved with 4-(4′-Phenoxyanilino)-6,7-dimethoxyquinazolinee (SKI-1), which is a recently developed potent, selective, dual site, and competitive inhibitor of Src kinase (25). The results would

Received 1/4/09; revised 2/16/09; accepted 2/23/09; published OnlineFirst 6/2/09.
Grant support: CRGC 10206721 and small project funding 200707176118 awarded by University of Hong Kong.
The costs of publication of this article were defrayed in part by the payment of page charges. This article must therefore be hereby marked *advertisement* in accordance with 18 U.S.C. section 1734 solely to indicate this fact.
Requests for reprints: Maria P. Wong, Department of Pathology, University of Hong Kong, Queen Mary Hospital, Pokfulam Road, Hong Kong. Phone: 852-2859-4861; Fax: 852-2872-5197. E-mail: mwpik@hkucc.hku.hk

doi:10.1158/1541-7786.MCR-09-0003

provide useful information for the development of targeted therapy for NSCLC, especially combinational regiments against TKI resistance.

Results

Src was Activated in NSCLC Cell Lines with EGFR Mutation and/or Amplification

EGFR and Src activation were studied by immunoblot analysis in seven human NSCLC cell lines with different EGFR mutations. Figure 1A showed that phosphorylated EGFR was observed in NSCLC cells with EGFR mutations or amplification but rarely in cells with wild-type (WT) EGFR. Interestingly, cells showing EGFR phosphorylation also showed Src phosphorylation; however, the degree of Src phosphorylation was not proportional to the level of EGFR phosphorylation. Quantitative analysis of the densitometric band intensity of phosphorylated Src normalized to total Src and actin showed that phosphorylated Src kinase levels at Y416 were significantly higher in NSCLC cells that harbored *EGFR* mutations and/or amplification including exon 19 deletion (HKULC3), L858R substitution (FA31), L858R+T790M double substitution (H1975), concomitant exon 19 deletion and amplification (HCC827), and amplification (H1819). H358 and HKULC2, which harbored WT-EGFR,

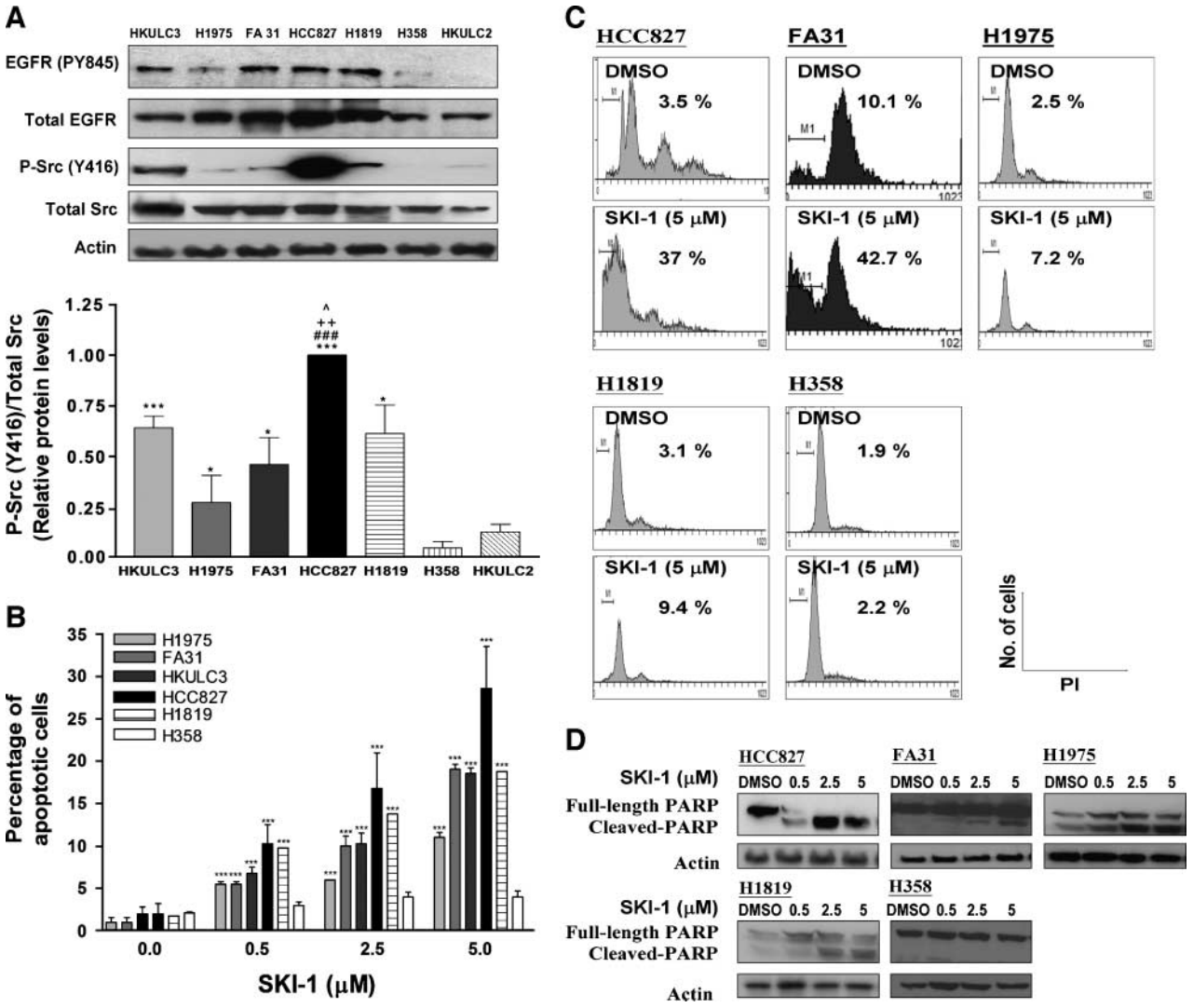

FIGURE 1. Western blot analysis of EGFR and Src, graphical representation of basal Src kinase activation levels and the apoptotic response to SKI-1 among a panel of serum-starved NSCLC cell lines. **A.** Total and phosphorylated EGFR and Src expression were shown by immunobloting. Graphically, cells harboring EGFR mutations (HKULC3, H1975, and FA31) and/or amplifications (HCC827 and H1819) showed significantly higher p-Src expression compared with cells with WT EGFR (H358and HKULC2). Columns, mean of expression ratio from four independent experiments normalized to actin loading; bars, SE. The densitometrical signal intensity of HCC827 was used as the standard (expression ratio, 1). *, $P < 0.05$, expression ratio compared with those of H358 and HKULC2; ***, $P < 0.001$ compared with H358 and HKULC2; ^, $P < 0.05$ compared with HKULC3; ###, $P < 0.001$, compared with H1975; ++, $P < 0.01$, compared with FA31. **B.** Apoptotic cells were quantified after Hoechst nuclear staining. Columns, mean of apoptotic cell percentage from four independent experiments; bars, SE. ***, $P < 0.001$ compared with the vehicle control group. **C.** Flow cytometry analysis of apoptotic cells before and after SKI-1 treatment, showing increased percentages of sub G_1 phase apoptotic cells (*horizontal bars*) in EGFR mutant but not WT cells. **D.** PARP cleavage analysis for apoptosis in cells treated with increasing dosages of SKI-1. The results shown were representative of four individual experiments.

showed almost no constitutive Src activation. Furthermore, cells with *EGFR* amplification showed stronger Src activation levels compared with those without. This was shown by the higher p-Src level in HCC827 compared with HKULC3, and in H1819 compared with H358 and HKULC2.

SKI, SKI-1 Induced Apoptosis in Cell Lines with EGFR Mutation and Amplification in a Dose Dependent Manner

To assess whether NSCLC cells were sensitive to SKI-1, cells with different *EGFR* status were exposed to increasing concentration of SKI-1 and quantitatively evaluated for apoptosis levels using Hoechst 33258 nuclear staining, flow cytometry for sub-G_1 proportion, and Poly (ADP-ribose) polymerase (PARP) cleavage analyses. Hoechst 33258 nuclear staining showed that 0.5 μmol/L or more of SKI-1 significantly induced apoptosis in the *EGFR* mutants H1975, FA31, HKULC3, HCC827, and H1819 in a dose-dependent manner, whereas the WT H358 was SKI-1 resistant (Fig. 1B). Using flow cytometric analysis of propidium iodide–labeled cancer cells, 0.5 μmol/L SKI-1 induced 37%, 42.7%, and 7.2% apoptotic cells, representing 10.6-, 4.2-, and 2.9-fold increases above the vehicle controls in HCC827, FA31, and H1975 cells, respectively. SKI-1 induced 9.4% (3.0-fold increase) of apoptotic cells in H1819 but had no effect on H358 (Fig. 1C). Furthermore, in HCC827 cells, PARP was completely cleaved by 2.5 μmol/L SKI-1, whereas cleavage increased with SKI-1 up to 10 μmol/L dosage but remained incomplete in H1975, FA31, and H1819 cells. Under the same dose range, the WT-EGFR H358 showed resistance to SKI-1 with no observable cleavage (Fig. 1D). Thus, results of apoptosis analysis by the different methods agreed with one another and showed that NSCLC cells with higher basal Src kinase phosphorylation were more sensitive to SKI-1 treatment. HCC827 and H1819 also showed higher apoptotic response than other respective *EGFR* mutant or WT cells without amplification.

Src and Src Direct Substrate Promoted Cell Migration and Invasion in SKI-Sensitive Cells

To show the role of Src in regulating cell motility, Matrigel invasion (Fig. 2A) and cell migration (Fig. 2B) assays were done by quantifying the ratio of the migrant cell foci in 5μmol/L SKI-1–treated compared with untreated controls. SKI-1 significantly inhibited cell invasion and migration in the SKI-sensitive HCC827 cells in a dose-dependent manner, whereas no effects were observed in H358 cells. Because the effect of Src on tumor metastasis/invasion is known to signal through the direct substrates FAK and p130Cas, the phosphorylation levels of these molecules were examined. After incubation with SKI-1 for 24 hours, reduction in phosphorylation levels of FAK and p130Cas were observed in the SKI-sensitive HCC827 and H1819 cells in a dose-dependent manner, whereas no change was observed in SKI-resistant H358 cells (Fig. 2C).

Validation of SKI-1 Specificity by siRNA-Induced Src Depletion

In HCC827 cells, 50 and 100 nmol/L siRNA tranfection achieved partial and complete inhibition of total Src protein expression, respectively. Src depletion also induced apoptosis as shown by PARP cleavage (Fig. 3A). To further study the specificity of SKI-1 inhibition on Src activation, the effect of increasing concentrations of SKI-1 on apoptosis and p-Src at different levels of siRNA knockdown was studied in HCC827 cells. In cells treated with either 50 or 100 nmol/L control siRNA, the total Src levels remained the same, whereas p-Src diminished with increasing concentrations of SKI-1 treatment. With partial suppression of Src expression by 50 nmol/L Src siRNA, indicated by the decreased total Src level, p-Src also diminished with increasing SKI-1 concentrations. However, when Src was completely suppressed after 100 nmol/L Src siRNA treatment, p-Src was undetectable with or without SKI-1 treatment (Fig. 3B, *top*). Similarly, when the response in the sub-G_1 cell population was measured, no further increase in the apoptotic fraction was observed in cells with total Src suppression compared with nonsupressed or partially suppressed cells (Fig. 3B, *bottom*). These results showed the dose-dependent suppressive effect of SKI-1 on Src activation and implicated that the apoptotic effect of SKI-1 was specifically mediated through Src kinase inhibition. Thus, SKI-1 could act as a specific pharmacologic inhibitor of Src kinase.

SKI-1 Differentially Inhibited Phosphorylation of Src, EGFR, and EGFR Downstream Effectors in Cells with Different EGFR Mutation Status

The effect of SKI-1 treatment on Src phosphorylation was studied using increasing doses of SKI-1 treatment. As shown in Fig. 4A, the strong pretreatment levels of Src phosphorylation were almost completely inhibited by 2.5 μmol/L SKI-1 in both HCC827 and H1819. For H358 cells, Src phosphorylation remained low and unchanged throughout this treatment dose, consistent with results of apoptosis studies which showed SKI resistance of H358 cells. To investigate the differential effects of SKI-1 in relation to *EGFR* genomic status, the phosphorylation profiles of EGFR and its downstream effectors were examined. Figure 4B showed that in both H1819 and HCC827, treatment with SKI-1 for 3 hours led to inhibition of EGFR phosphorylation at Y845, Y1086, and Y1173 in a dose-dependent manner. This inhibitory effect on EGFR phosphorylation was also observed by Src depletion using siRNA (Fig. 3A). Correspondingly, the phosphorylation of EGFR downstream effectors including p-STAT 3 (S727, Y705), p-p42/44 ERK1/2 (T202/Y204), and p-Akt (S473) proteins were inhibited by SKI-1 treatment (Fig. 4C). In H358 cells with low basal Src and EGFR phosphorylation levels, no change was induced by SKI-1 treatment. The results indicated that SKI-1–induced apoptosis in both H1819 and HCC827 cells involved the EGFR downstream antiapoptotic signaling cascade.

SKI-1 and Gefitinib Enhanced Apoptosis in NSCLC Cells

To investigate the cotreatment effect of SKI-1 and gefitinib, we compared the levels of apoptosis after single or combined SKI-1 and/or gefitinib in cancer cells with different EGFR mutations. The apoptosis levels were analyzed by Hoechst staining and PARP cleavage after 24 hours of drug treatment. In FA31, which harbored L858R, both gefitinib and SKI-1 significantly induced apoptosis. Under combination treatment, apoptosis was enhanced significantly (Fig. 5A). Using similar dosages for H1819 treatment, gefitinib alone did not induce apoptosis to a significant level compared with nontreated

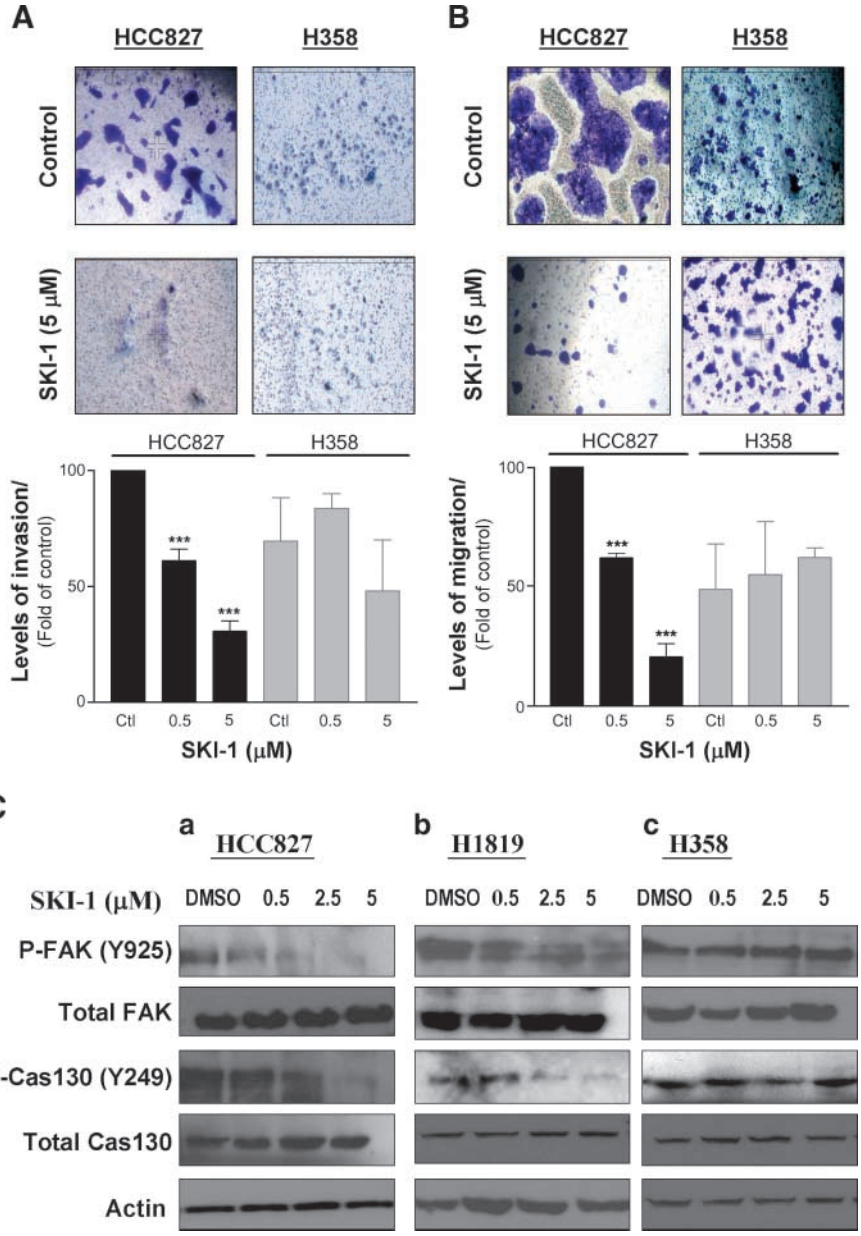

FIGURE 2. Involvement of Src and Src direct substrates in cell migration and invasion of SKI-sensitive NSCLC cells. **A.** HCC827 cells were SKI-1 treated and allowed to invade through a Matrigel-coated insert or (**B**) migrate through a serum-free medium-coated insert for 48 h. Top, representative micrographs showing cell colonies on the lower surface of the insert membrane. Bottom, the number of invading and migrating colonies were counted and compared with vehicle controls. Columns, mean of three individual experiments; bars, SE; ***, $P < 0.001$ compared with HCC827 untreated group. **C.** SKI-1-treated HCC827, H1819, and H358 cells were lysed and analyzed for FAK and Cas130 Src substrates by immunoblotting. Western blots are representative of three independent experiments.

controls, whereas SKI-1 alone induced significant apoptosis. Cotreatment with gefitinib enhanced apoptosis and PARP cleavage compared with treatment with either drug alone (Fig. 5B). In H1975, no effects were induced by gefitinib alone; SKI-1 treatment resulted in significantly increased apoptosis, although the levels of apoptosis were modest. However, additive effects were not observed by the combination of these drugs (Fig. 5C).

Immunohistochemistry Analysis of p-Src and EGFR Expression in Clinical Lung Cancers

The pattern of Src phosphorylation and EGFR expression were studied in totally 187 adenocarcinomas and squamous cell carcinomas (SCC) with known *EGFR* genomic status. The results were presented in Supplementary Table S1. Medium to high levels of Src phosphorylation were found in 28.3% (53 of 187) of lung tumors. P-Src levels correlated with EGFR expression when tumors were stratified into none/low-expression (grade 0-1) and medium/high-expression groups (grade 2-3; $P = 0.025$). Stronger EGFR expression was more often observed in SCCs compared with adenocarcinomas ($P = 0.012$). Stage T1 tumors more often showed stronger p-Src expression ($P = 0.007$). No significant association was observed between p-Src or EGFR expression with other clinical and pathologic parameters including smoking history, gender, age, lymph node or pathologic stages, and *EGFR* mutational profile. When only adenocarcinomas was considered, *EGFR* mutant tumors more often showed p-Src expression (37 of 88; 42.0%) than the WT tumors (16 of 64; 25.0%; $P = 0.029$). No correlation between EGFR expression and mutations was found. No other significant association between p-Src or EGFR

expression and clinicopathologic parameters was observed in adenocarcinomas. Representative immunohistochemistry (IHC) cases were shown in Fig. 6A and B.

Discussion

This study investigated whether Src kinase is a potential drug target for treating NSCLC. The basal Src phosphorylation levels and effects of Src inhibition were shown in a panel of lung cancer cell lines including those raised from Chinese patients with different known *EGFR* genomic statuses. The pattern of p-Src expression was also immunohistochemically analyzed in a panel of primary human lung cancers from local patients. SKI-1, a competitive dual-site Src inhibitor, which simultaneously interacts with both the ATP- and peptide-binding sites, was used to inhibit Src kinase (25). SKI-1 treatment led to apoptosis of selective cancer cell lines and the observations were verified by specific siRNA knock-down studies.

NSCLC cells with *EGFR* mutations showed higher basal p-Src levels than those with WT-EGFR due to the mutual activation of EGFR and Src, with increased apoptosis response induced by SKI-1 treatment. The findings agree with other reported studies that used alternative molecular or conventional SKIs such as Dasatinib and propidium iodide (22, 23). Because these drugs could have nonspecific actions affecting other kinases such as EGFR, PDGFR, kit, Abl, etc. (22, 26), the use of Src-specific inhibitor in our study provides more definitive support that the Src pathway is engaged in the survival of lung cancer cells with *EGFR* aberrations. Similar to Amann et al. (27) and Okabe et al. (28), we found that HCC827, which harbors both high level *EGFR* amplification and exon 19 deletion, showed a much higher basal p-Src level and enhanced SKI-1 response than cells with other types of *EGFR* mutations such as exon 19 deletion alone (HKULC3), L858R alone (FA31), or L858R concurrent with T790M (H1975). PC9, another lung cancer cell line that harbors *EGFR* amplification, is also reported to show similar responses (22). Our results also showed enhanced Src phosphorylation and SKI-1 sensitivity in H1819, which is reported to show low level amplification (5.3 copies per cell) of WT *EGFR* with high ErbB2 and ErbB3 expression (27-29). Our chromogenic *in situ* hybridization analysis on H1819 cells showed only three to four *EGFR* signals per cell,

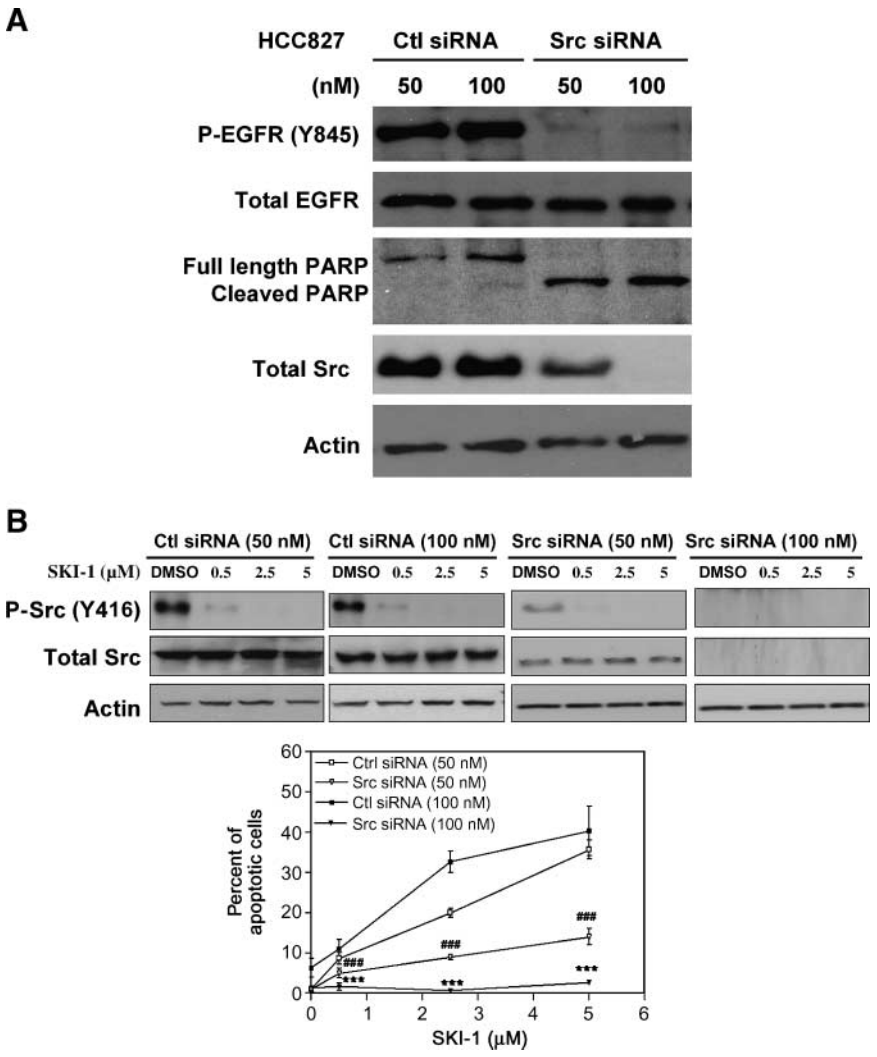

FIGURE 3. Specific anti-Src action of SKI-1 shown by siRNA-mediated Src depletion. **A.** Effect of Src knockdown on EGFR phosphorylation and apoptosis in HCC827 cells. Cells were transfected with specific Src siRNA or nontargeting control siRNA (*ctl siRNA*) at 50 and 100 nmol/L for 72 h. Cell lysates were analyzed for EGFR (Y845) phosphorylation, PARP cleavage, and Src expression. Western blots were representative of three independent experiments. **B.** Effect of Src knockdown and inhibition on p-Src expression and apoptosis in HCC827 cells. Src depletion was done as described in **A** using 50, 100 nmol/L of Src siRNA or nontargeting (control) siRNA, respectively, followed by incubation for 24 h in the presence or absence of SKI-1 at a concentration range of 0.5, 2.5, and 5 μmol/L. Harvested cells were lysed for Western blot analysis or stained with propidium iodide for analysis by flow cytometry. The relation between SKI-1 concentrations and percentages of apoptotic cells at sub-G_1 phase was presented as a dose-response curve. ###, $P < 0.001$, compared with control siRNA (50 nmol/L) group; ***, $P < 0.001$ compared with control siRNA (100 nmol/L) group.

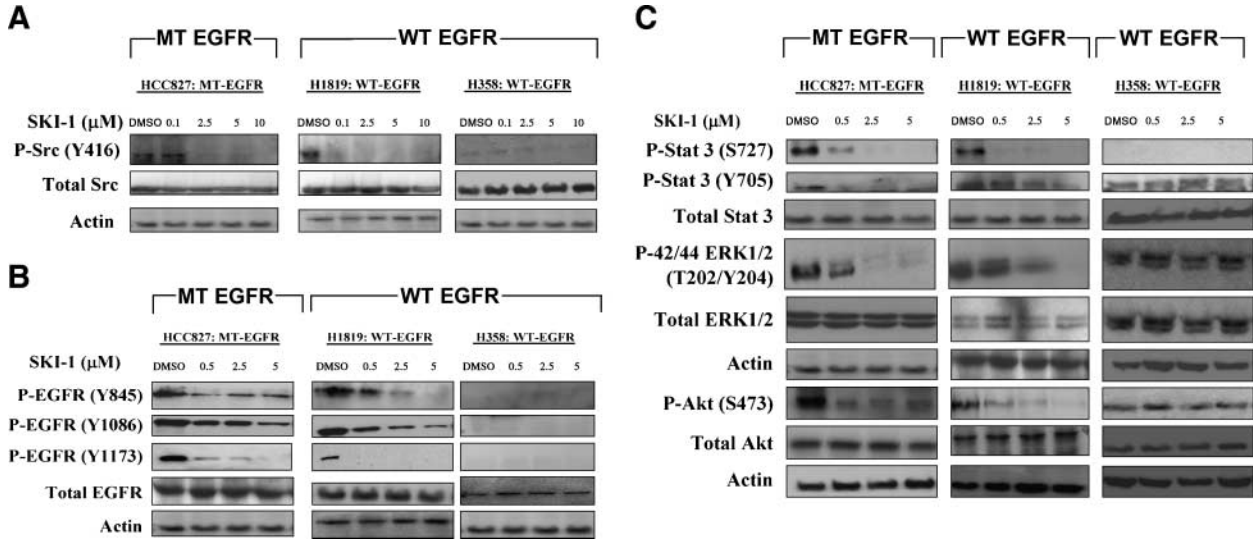

FIGURE 4. Effect of SKI-1 treatments on phosphorylation profiles in sensitive and resistant cells. HCC827, H1819, and H358 cells were serum starved for 24 h and incubated with SKI-1 for 3 h. Western blots are representative of three independent experiments. **A.** Src phosphorylation profiles. **B.** EGFR phosphorylation profiles. **C.** EGFR downstream effectors profiles.

but IHC analysis showed strong ErbB2 expression (data not shown). ErbB2-induced Src activation has been shown in rodent mammary tumors and transformed mammary epithelial cells (30, 31). Also, ErbB2-mediated recruitment of Src to ErbB2/EGFR heterodimers has been suggested as a critical step in EGFR transphosphorylation (32), suggesting that Src could be activated by high ErbB2 levels. Together, the findings suggest that Src activation by enhanced mutant or WT *EGFR* and *EGFR* family receptor signaling could play a role in lung cancer cell survival.

The molecular mechanisms and effects of SKI treatment on lung cancer cells are incompletely understood. The major EGFR autophosphorylation sites (Y992, Y1068, Y1086, Y1148, and Y1173) for both WT (33, 34) and mutant *EGFR* (15, 16) are located within the kinase domain. However, it has been shown *in vitro* and *in vivo* that Src kinase directly and uniquely phosphorylates EGFR at Y845 (5, 35), which is located outside the kinase domain, unlike equivalent sites of other receptor tyrosine kinases such as CSF-1-R, HGFR, and FGFR (36). Under serum-starvation, both HCC827 and H1819 cells showed EGFR phosphorylation and SKI-induced inhibition at Y845. However, markedly reduced pY1086 and pY1173 were also observed, suggesting that indirect Src-related pathways could also be involved in EGFR phosphorylation.

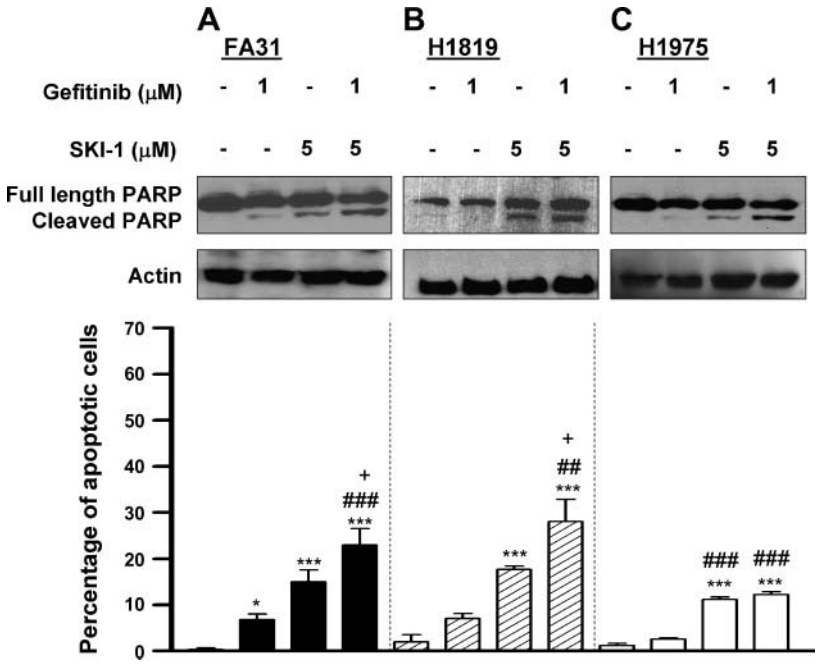

FIGURE 5. Apoptotic effects of single or combined SKI-1 and/or Gefitinib treatment. FA31, H1819, and H1975 cells were serum-depleted for 24 h and incubated with single or combined SKI-1 and/or Gefitinib for 24 h. Top, representative Western blot for PARP cleavage analysis. Western blots are representative of three independent experiments. Bottom, percentage of apoptotic cells semiquantitatively measured by Hoechst staining. Columns, mean of three individual experiments; bars, SE. **A.** FA31 cells; * and ***, $P < 0.05$ and $P < 0.001$, respectively, compared with the vehicle control group; +, $P < 0.05$ compared with SKI-1 alone group; ###, $P < 0.001$ compared with Gefitinib alone group. **B.** H1819 cells; ***, $P < 0.001$ compared with the vehicle control group; +, $P < 0.05$ compared with Gefitinib alone group; ##, $P < 0.01$ compared with SKI-1 alone group. **C.** H1975 cells; ***, $P < 0.001$ compared with the vehicle control group; ###, $P < 0.001$ compared with Gefitinib-treated group.

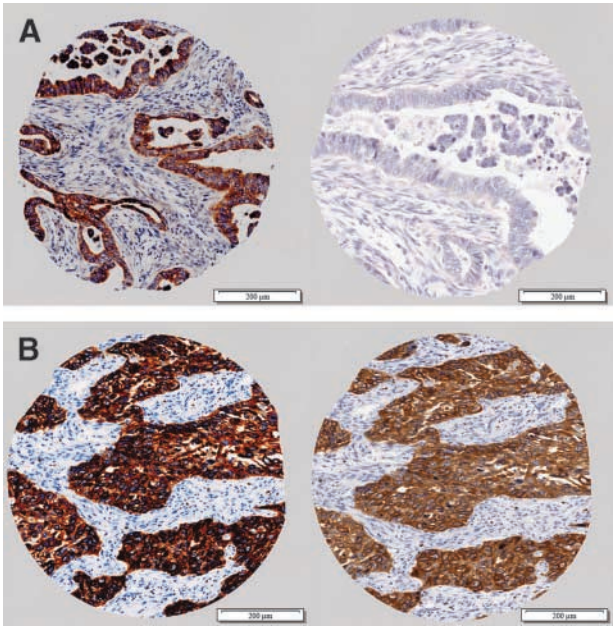

FIGURE 6. Immunohistochemical analysis of p-Src and EGFR expression levels in two representative NSCLC tissue array cores. **A.** Example of strong cytoplasmic p-Src (*left*) and nil EGFR (*right*) staining in a stage 3A adenocarcinoma with *EGFR* L858R mutation from a female passive smoker. **B.** Example of strong p-Src (*left*) and strong cell membrane EGFR (*right*) expression in a stage 3B squamous cell carcinoma with wild-type EGFR from a male smoker.

One candidate of such an interaction consists of Src-integrin association, which has been shown to induce EGFR Y845, Y1086, and Y1173 phosphorylation (37). Thus, SKI treatment alone could inhibit phosphorylation of these sites, leading to cell apoptosis due to suppression of EGFR downstream mediator(s) including AKT (downstream of Y1086), p42/44 ERK1/2 (downstream of pY1173), and STAT3/5 (downstream of Y845; Fig. 5C; refs. 15, 16). This provides additional inhibitory action over that by gefitinib treatment alone because the latter reduces Stat and Akt but not ERK1/2 phosphorylation (16). Furthermore, our results of SKI-1 treatment of HCC827 and H1819 also showed inhibition of the FAK and p130C Src direct substrates, which are EGFR-independent signaling pathways involved in cell invasion and migration (1, 38, 39). Thus, targeting Src would provide extra treatment benefits in addition to induction of apoptosis.

Recently, additive effects of gefitinib and PP1 cotreatment has been shown in H3255 cells (L858R substitution) leading to decreased cell proliferation, and in HCC827 cells with additional enhancement of apoptosis (23). In this study, we have also shown the enhanced apoptotic effects of SKI-1 and gefitinib in another cell line with L858R substitution (FA31), which was raised from the malignant pleural effusion of a Chinese smoker with lung adenocarcinoma. H1819 cells have been reported to show only moderate sensitivity to gefitinib due to absence of *EGFR* mutation with an IC_{50} value of 4.7 μmol/L (27). In our study, gefitinib alone did not induce significant apoptosis but cotreatment with SKI-1 enhanced the apoptotic fraction to significant levels compared with untreated controls or gefitinib-treated cells. In fact, both cell lines showed high levels of endogenous Src phosphorylation, which might be explained by mutual activation with EGFR; the activated Src could further enhance its own activity by autophosphorylation in an EGFR-independent manner (2, 3). These cells might become partially dependent on Src for survival in addition to EGFR, so that applying gefitinib alone targeting EGFR could not inhibit Src-mediated survival pathways completely. H1975 cells were resistant to gefitinib due to steric hindrance caused by T790M. However, SKI-1 alone was able to induce significant apoptosis, which was not further enhanced by gefitinib and SKI-1 cotreatment, illustrating an oncogenic role of Src, which was independent of EGFR activation. Despite the modest levels of apoptosis induced, which was consistent with the findings of Song et al. (22) and Zhang et al. (23) who used different Src inhibiting agents, the findings implicated that targeting Src kinase could be an alternative treatment method for patients resistant to TKI due to concomitant T790M mutation. Further studies are required to evaluate the treatment outcome in clinical situations.

Src expression has been reported in many tumors, but as far as we can trace from the literature, only three studies have shown p-Src expression using immunohistochemical or Western blot approaches in clinical lung cancers, including 1 study of 30 tumors from Japan (9) and 2 from Western countries involving 33 and 370 lung cancer cases, respectively (11, 23). In our study, activated Src expression was found in 28.3% and EGFR in 21.4% of the 187 samples. The data are comparable with those from other large scale IHC studies. For example, Zhang et al. (23) showed activated Src expression in 33.2% of 370 lung cancers, whereas Hirsch et al. (40) found EGFR expression in 22% of 379 samples. Jeon et al. (41) studied a larger number of 262 lung cancers and found a higher EGFR expression rate of 53.1%, and close association of EGFR expression with SCC ($P < 0.001$) was also shown. In contrast to our findings, Zhang et al. (23) showed correlation of p-Src with male, active smoker and SCC tumor type. This difference could be related to the inclusion of many more adenocarcinomas than SCC in our samples for the comparison of *EGFR* mutant and WT tumors. To our knowledge, although *EGFR* gene sequence changes have been investigated in many studies, large-scale comparisons of p-Src and EGFR expression with *EGFR* mutation status have not been reported thus far. In our data, when the tumors were stratified into none/low-expression (grade 0-1) and medium/high-expression (grade 2-3) groups, a positive correlation between p-Src and EGFR expression was apparent. Although the statistical association was weakly significant ($P = 0.025$), the observations nevertheless lent support to the Src and EGFR signaling relation modeled in our cell line studies. Various other factors not assessed in our IHC study might regulate p-Src protein expression and affect the staining intensities, such as *EGFR* gene amplification and other biological factors involved in Src signaling cascades. In the adenocarcinoma group, tumors showing *EGFR* mutations more often showed Src phosphorylation, but the intensity of expression varied from weak to strong, suggesting that other factors could also affect the level of Src activation.

Taken together, the present study provides information on the role of Src and its interaction with EGFR pathway in lung cancers. The results indicate that *EGFR* mutations and possibly

other abnormalities of EGFR and related family members leading to enhanced Src expression are important determinants of tumor sensitivity to SKI. Inhibition of the Src pathway alone could be beneficial in inducing apoptosis and combined treatment with gefitinib could further enhance the proapoptotic drug actions in tumors with EGFR and/or HER2 abnormalities.

Materials and Methods

Culture of Established Cell Lines of Human NSCLC

Seven established human NSCLC cell lines, HKULC2, HKULC3, H358, H1819, HCC827, FA31, and H1975 cells were used. The establishment and characteristics of HKULC2 and HKULC3 had been previously described (42). FA31 was derived from the metastatic pleural effusion of an 83-y-old female Chinese patient with lung adenocarcinoma without prior chemotherapy. EGFR sequencing analysis of the tumor cells showed L858R substitution. All three local cell lines showed no *EGFR* amplification. Other cell lines were purchased from American Type Culture Collection. They were cultured in RPMI 1640 at 37°C, 5% CO_2/95% air. All media were supplemented with fetal bovine serum (10%), streptomycin (50 μg/mL), and penicillin (50 units/mL).

Drug Treatment on NSCLC Cells

Cells (2×10^5) were seeded in 6-well plates and allowed to attach. Cells were then starved for 24 h and treated with drugs for 24 h for apoptosis studies or 3 h preblocking for Src, EGFR, and downstream effectors phosphorylation profile studies. Cells were treated with the vehicle (DMSO) as the control groups.

Hoechst 33258 Staining

After experimental treatments, cells were trypsinized, both attached and floating cells were pooled, then pelleted by centrifugation, and resuspended in phosphate buffered formalin (10%) containing Hoechst 33258 (12.5 ng/mL). Cells were spotted onto slides for microscopy. Nuclear staining was observed and photographed using a fluorescence microscope (magnification, ×400). Cells with typical apoptotic nuclear morphology, including nuclear shrinkage, condensation, and fragmentation, were identified and counted as previously reported (43) based on random fields selection. The counter was "blinded" to sample identity to avoid experimental bias and at least 200 cells were counted in each treatment group.

Flow Cytometry

After treatment, cell suspensions were fixed with 70% ethanol overnight. Fixed cells were then resuspended in PBS containing 0.02 mg/mL propidium iodide and 0.2 mg/mL DNase-free RNase A in the dark for 30 mins. Cell cycle profiles were analyzed by a FACSort flow cytometry (BD Calibur) with Wi nmol/L DI 2.8 software (The Scripps Institute). Apoptotic cells were determined by the percentage of events accumulated in sub-G_1 phase proportion. The total number of counted events was the same for each cell line studied.

Matrigel Invasion and Migration Assay

Cell invasion and migration assays were preformed in Boyden chambers with growth factor–depleted Matrigel-coated membrane filters with a pore size of 8 μmol/L (BD Bioscience). Cells (2×10^5) were loaded onto the top chamber and medium with 10% fetal bovine serum in the bottom chamber. Cells were allowed to invade or migrate through a Matrigel-coated insert (for invasion study) or serum-free medium-coated insert (for migration study). After 48 h, the invaded or migrated cells were fixed with 100% methanol and stained with 0.5% crystal violet. The number of cells that had invaded was photographed by random selection of 5 fields (×20) of each membrane and quantitatively assessed by reading absorbance at 560 nm after redissolving crystal violet staining with 10% acetic acid.

Protein Extraction and Western Blot Analysis

Cells were lysed in ice-cold lysis buffer (pH 7.4) containing 50 mmol/L Hepes, 150 mmol/L NaCl, 1.5 mmol/L $MgCl_2$, 1 mmol/L ethylene glycol tetraacetic acid, 100 mmol/L NaF, 10 mmol/L NaPPi, 10% Glycerol, and 1% Triton X-100. The protease inhibitors phenylmethylsulfonyl fluoride (10 μmol/L), protease inhibitor cocktail (1: 50; Sigma), and phosphatase inhibitor cocktail (1: 50; Sigma) were added to the lysis buffer freshly. The cell lysate was syringed briefly for 20 times on ice, incubated on ice for 1 h, and pelleted by centrifugation (13,000 × *g*; 20 min). The supernatant was collected as a whole-cell lysate and stored at −20°C. Protein concentration was determined using Bio-Rad detergent-compatible protein assay kit. Equal amounts of proteins (50-100 μg) were loaded and resolved by 10% SDS-PAGE and electro-transferred (30V; 16 h) onto nitrocellulose membranes (Bio-Rad). Membranes were blocked (room temperature, 1 h) with Blocking buffer [Tris-HCl (10 mmol/L; pH 8.0), NaCl (150 mmol/L), Tween 20 (0.05%, v/v; TBS-Tween 20) containing bovine serum albumin (5%; w/v)], then incubated overnight with specific primary antibodies (1: 1,000 dilution) and subsequently with the appropriate horseradish peroxidase–conjugated secondary antibody [1:2,000 in 5% bovine serum albumin blocking; room temperature for 1 h]. The primary antibodies included p-Src (Y416), total Src, PARP, p-FAK (Y925), total FAK, p-Cas130 (Y249), total Cas130, p-EGFR (Y845), p-EGFR (Y1086), p-EGFR (Y1173), total EGFR, p-STAT3 (S727), p-STAT3 (Y705), total STAT3, p-ERK1/2 (T202/Y204), total ERK1/2, p-AKT (S473), total AKT, and total actin (Cell signaling Technologies). The membranes were then washed with TBS-Tween 20 thrice (15 min per wash), and peroxidase activity was visualized with enhanced chemiluminescence (Amersham) reagent (Amersham Biosciences) or enhanced chemiluminescence plus reagent (Amersham Biosciences), and exposed to Hyperfilm enhanced chemiluminescence (Amersham Biosciences). Signal intensity was quantitatively determined densitometrically by NIH ImageJ version 1.36b software.[5]

RNA Interference

SRC siRNA (Ambion) and nontargeting siRNA (DHARMACON) were mixed with RiboJuice (Novagen) to final concentrations of 50 or 100 nmol/L, respectively. After plating cells for 18 h, the siRNA mixture was added drop by drop to each well to ensure maximal coverage, and an additional 1,250 μL of complete media were added to bring the total volume to 1.5 mL. The cells were incubated for 72 h and then the

[5] http://rsb.info.nih.gov/ij

medium was replaced. Down-regulation was confirmed by Western blot analysis.

Immunohistochemistry of Clinical Specimen

Resected tumors of 187 primary NSCLC from local Chinese patients without prior radiotherapy or chemotherapy were studied for p-Src and EGFR expression using IHC. Tumor cores of 0.6-mm diameter in 3 to 4 replicates were arrayed on tissue array blocks that included control tissues from normal lung, stomach, liver, uterus, and a constant sample of lung carcinoma to enable comparison of staining intensities among different tissue array blocks. Only tumors that showed moderate to strong expression of general cytokeratin markers were included to ensure optimal tissue preservation. Tumor typing and staging criteria and definitions of smoking history were as previously described (13). Deparaffinized sections blocked for biotin and peroxidase were labeled with anti–p-Src antibodies against Y416 (Cell Signaling Technologies) at 1: 50 dilution overnight at 4°C. Although this antibody has been recommended for immunoblot studies, optimization for IHC studies have been reported (44). Biotinylated goat anti-rabbit secondary antibody at 1:200 dilution was added followed by streptavidin-peroxidase complex at 1:100 dilution (DAKO). Detection was done by incubating slides with substrate 3,3′-diaminobenzidine (Amresco) and peroxide. The slides were then rinsed and counterstained with hematoxyline, rinsed, dehydrated, and mounted. In the control slide, the primary antibody was replaced with 10% normal goat serum. EGFR expression was analyzed using the EGFR pharmDx kit (DAKO) according to the recommendation of the manufacturer. Images of stained sections were acquired by the Aperio automated slide scanner and image analysis system (Aperio). The expression levels of both Src and EGFR were classified as grades 1 to 3 according to the intensity and tumor proportion of staining according to the recommendations used for EGFR grading.

Statistical Analysis

Statistical analysis was carried out by ANOVA (GraphPad PRISM software version 3.0). Differences between experimental groups were determined by the Newman-Keuls test for basal Src, apoptosis, invasion, and migration levels. Statistical analysis of IHC results and comparison with clinicopathologic data were done by the χ^2 test using SPSS version 16.0 (SPSS, Inc.). The 2-sided significance level was set at a P value of <0.05.

Disclosure of Potential Conflicts of Interest

No potential conflicts of interest were disclosed.

Acknowledgments

We thank Dr. Elaine Wang, Department of Pathology, Grantham Hospital, and all surgeons of the Cardiothoracic Unit of Queen Mary Hospital, Hong Kong, for sample procurement and collection of clinical data, and AztraZaneca for providing Gefitinib in this study.

References

1. Parsons SJ, Parsons JT. Src family kinases, key regulators of signal transduction. Oncogene 2004;23:7906–9.

2. Roskoski JR. Src protein-tyrosine kinase structure and regulation. Biochem Biophys Res Commun 2004;324:1155–64.

3. Roskoski JR. Src kinase regulation by phosphorylation and dephosphorylation. Biochem Biophys Res Commun 2005;331:1–14.

4. Irby RB, Yeatman TJ. Role of Src expression and activation in human cancer. Oncogene 2000;19:5636–42.

5. Egan C, Pang A, Durda D, Cheng HC, Wang JH, Fujita DJ. Activation of Src in human breast tumor cell lines: elevated levels of phosphotyrosine phosphatase activity that preferentially recognizes the Src carboxy terminal negative regulatory tyrosine 530. Oncogene 1999;18:1227–37.

6. Cartwright CA, Coad CA, Egbert BM. Elevated c-Src tyrosine kinase activity in premalignant epithelia of ulcerative colitis. J Clin Invest 1994;93:509–15.

7. Wiener JR, Nakano K, Kruzelock RP, Bucana CD, Bast RC, Jr., Gallick GE. Decreased Src tyrosine kinase activity inhibits malignant human ovarian cancer tumor growth in a nude mouse model. Clin Cancer Res 1999;5:2164–70.

8. Takeshima E, Hamaguchi M, Watanabe T, et al. Aberrant elevation of tyrosine-specific phosphorylation in human gastric cancer cells. Jpn J Cancer Res 1991;84: 1428–35.

9. Masaki T, Igarashi K, Tokuda M, et al. pp60c-src activation in lung adenocarcinoma. Eur J Cancer 2003;39:1447–55.

10. Mazurenko NN, Kogan EA, Zborovskaia IB, Sukhova NM, Kiselev FL. The detection of the c-src protein gene product in human lung tumors. Vopr Onkol 1991;37:683–90.

11. Mazurenko NN, Kogan EA, Zborovskaya IB, Kisseljov FL. Expression of pp60c-src in human small cell and non-small cell lung carcinomas. Eur J Cancer 1992;28:372–7.

12. Huang SF, Liu HP, Li LH, et al. High frequency of epidermal growth factor receptor mutations with complex patterns in non-small cell lung cancers related to gefitinib responsiveness in Taiwan. Clin Cancer Res 2004;10:8195–203.

13. Tam IYS, Chung LP, Suen WS, et al. Distinct epidermal growth factor receptor and KRAS mutation patterns in non-small cell lung cancer patients with different tobacco exposure and clinicopathologic features. Clin Cancer Res 2006; 12:1647–53.

14. Gazdar AF, Shigematsu H, Herz J, Minna JD. Mutations and addiction to EGFR: the Achilles 'heal' of lung cancers? Trends Mol Med 2004;10:481–6.

15. Lynch TJ, Bell DW, Sordella R, et al. Activating mutations in the epidermal growth factor receptor underlying responsiveness of non-small-cell lung cancer to gefitinib. N Engl J Med 2004;350:2129–39.

16. Sordella R, Bell DW, Haber DA, Settleman J. Gefitinib-sensitizing EGFR mutations in lung cancer activate anti-apoptotic pathways. Science 2004;305: 1163–7.

17. Engelman JA, Zejnullahu K, Mitsudomi T, et al. MET amplification leads to gefitinib resistance in lung cancer by activating ERBB3 signaling. Science 2007; 316:1039–43.

18. Pao W, Miller VA, Politi KA, et al. Acquired resistance of lung adenocarcinomas to gefitinib or erlotinib is associated with a second mutation in the EGFR kinase domain. PLoS Med 2005;2:e73.

19. Biscardi JS, Maa MC, Tice DA, Cox ME, Leu TH, Parsons SJ. c-Src-mediated phosphorylation of the epidermal growth factor receptor on Tyr845 and Tyr1101 is associated with modulation of receptor function. J Biol Chem 1999;274:8335–43.

20. Biscardi JS, Tice DA, Parsons SJ. c-Src, receptor tyrosine kinases, and human cancer. Adv Cancer Res 1999;76:61–119.

21. Bromann PA, Korkaya H, Courtneidge SA. The interplay between Src family kinases and receptor tyrosine kinases. Oncogene 2004;23:7957–68.

22. Song L, Morris M, Bagui T, Lee FY, Jove R, Haura EB. Dasatinib (BMS-354825) selectively induces apoptosis in lung cancer cells dependent on epidermal growth factor receptor signaling for survival. Cancer Res 2006;66: 5542–8.

23. Zhang J, Kalyankrishna S, Wislez M, et al. SRC-family kinases are activated in non-small cell lung cancer and promote the survival of epidermal growth factor receptor-dependent cell lines. Am J Pathol 2007;170:366–76.

24. Zheng R, Yano S, Matsumori Y, et al. Src tyrosine kinase inhibitor, M475271, suppresses subcutaneous growth and production of lung metastasis via inhibition of proliferation, invasion, and vascularization of human lung adenocarcinoma cells. Clin Exp Metastasis 2005;V22:195–204.

25. Tian G, Gory M, Smith AA, Knight WB. Structural determinants for potent, selective dual site inhibition of human pp60c-src by 4-anilinoquinazolines. Biochemistry 2001;40:7084–91.

26. Force T, Krause DS, Van Etten RA. Molecular mechanisms of cardiotoxicity of tyrosine kinase inhibition. Nat Rev 2007;7:332–44.

27. Amann J, Kalyankrishna S, Massion PP, et al. Aberrant epidermal growth factor receptor signaling and enhanced sensitivity to EGFR inhibitors in lung cancer. Cancer Res 2005;65:226–35.

28. Okabe T, Okamoto I, Tamura K, et al. Differential constitutive activation of the epidermal growth factor receptor in non-small cell lung cancer cells bearing EGFR gene mutation and amplification. Cancer Res 2007;67:2046–53.

29. Fujimoto N, Wislez M, Zhang J, et al. High expression of ErbB family members and their ligands in lung adenocarcinomas that are sensitive to inhibition of epidermal growth factor receptor. Cancer Res 2005;65:11478–85.

30. Fleming JM, Desury G, Polanco TA, Cohick WS. Insulin growth factor-I and epidermal growth factor receptors recruit distinct upstream signaling molecules to enhance AKT activation in mammary epithelial cells. Endocrinology 2006;147: 6027–35.

31. Muthuswamy SK, Muller WJ. Direct and specific interaction of c-Src with Neu is involved in signaling by the epidermal growth factor receptor. Oncogene 1995;11:271–9.

32. Kim H, Chan R, Dankort DL, et al. The c-Src tyrosine kinase associates with the catalytic domain of ErbB-2: implications for ErbB-2 mediated signaling and transformation. Oncogene 2005;24:7599–607.

33. Jorissen RN, Walker F, Pouliot N, Garrett TP, Ward CW, Burgess AW. Epidermal growth factor receptor: mechanisms of activation and signalling. Exp Cell Res 2003;284:31–53.

34. Sebastian S, Settleman J, Reshkin SJ, Azzariti A, Bellizzi A, Paradiso A. The complexity of targeting EGFR signalling in cancer: from expression to turnover. BBA 2006;1766:120–39.

35. Haskell MD, Slack JK, Parsons JT, Parsons SJ. c-Src tyrosine phosphorylation of epidermal growth factor receptor, P190 RhoGAP, focal adhesion kinase regulates diverse cellular processes. Chem Rev 2001;101:2425–40.

36. Tice DA, Biscardi JS, Nickles AL, Parsons SJ. Mechanism of biological synergy between cellular Src and epidermal growth factor receptor. Proc Natl Acad Sci U S A 1999;96:1415–20.

37. Moro L, Dolce L, Cabodi S, et al. Integrin-induced epidermal growth factor (EGF) receptor activation requires c-Src and p130Cas and leads to phosphorylation of specific EGF receptor tyrosines. J Biol Chem 2002;277: 9405–14.

38. Siesser PM, Hanks SK. The signaling and biological implications of FAK overexpression in cancer. Clin Cancer Res 2006;12:3233–7.

39. Vuori K, Hirai H, Aizawa S, Ruoslahti E. Introduction of p130cas signaling complex formation upon integrin-mediated cell adhesion: a role for Src family kinases. Mol Cell Biol 1996;16:2606–13.

40. Hirsch FR, Dziadziuszko R, Thatcher N, et al. Epidermal growth factor receptor immunohistochemistry: comparison of antibodies and cutoff points to predict benefit from gefitinib in a phase 3 placebo-controlled study in advanced nonsmall-cell lung cancer. Cancer 2008;112:1114–21.

41. Jeon YK, Sung SW, Chung JH, et al. Clinicopathologic features and prognostic implications of epidermal growth factor receptor (EGFR) gene copy number and protein expression in non-small cell lung cancer. Lung Cancer 2006;54: 387–98.

42. Lam DC, Girard L, Suen WS, et al. Establishment and expression profiling of new lung cancer cell lines from Chinese smokers and lifetime never-smokers. J Thorac Oncol 2006;1:932–42.

43. Wyllie AH. Glucocorticoid-induced thymocyte apoptosis is associated with endogenous endonuclease activation. Nature 1980;284:555–6.

44. Campbell EJ, McDuff E, Tatarov O, et al. Phosphorylated c-Src in the nucleus is associated with improved patient outcome in ER-positive breast cancer. Br J Cancer 2008;99:1769–74.